Performance Comparison of Low Current Measurement Systems for Biomedical Applications

Dongsoo Kim, Wei Tang, Brian Goldstein, Pujitha Weerakoon, Hazael Montanaro, Berin Martini, and Eugenio Culurciello
Department of Electrical Engineering
Yale University, CT USA
Email: dongsoo.kim@yale.edu, eugenio.culurciello@yale.edu

***Abstract*— In this paper, we report on the noise analysis of low current measurement systems for biomedical applications. We analyzed resistive feedback, capacitive feedback and current conveyor circuits for low current measurement systems. Detailed noise analysis are presented and matched with measurement data using a 0.5-μm fabrication process. Based on the theoretical analysis and the measurements, the capacitive feedback system provides better noise performance for the measurement of low current. The capacitive feedback is capable of measuring 700fA RMS at 10KHz sampling rate, whereas the resistive feedback provides 4pA and the current conveyor provides 600pA. This paper provides design guidelines to maximize the measurement performance of low current for biomedical instrumentation.**

I. Introduction

Integrated current measurement systems are becoming an extremely important integrated circuit component to interface and study physical phenomena at the sub-micro-scale and also for biological research and instrumentation [1]. All of these measurements require compact instrumentation head-stage with very low input current noise. For example, to measure ion channel and membrane protein currents, an integrated low current measurement system with pico-ampere resolution is required, such as commercial patch-clamp amplifiers.These amplifiers can measure the cell membrane conductance and are normally used to study the effect of drugs and medical treatments on ion channel dynamics. Another example of low current measurement system (LCMS) is used in DNA sequencing [2], where base pairs passing through nanopores can be detected with amperometric measurements. Several low current measurement systems have been implemented and published in the literature. Typical systems use an operational amplifier with capacitive [3] or resistive feedback [1] as a head-stage. Another approach is using current conveyor to amplify the input current [4].

LCMSs are designed to measure the input current, I_S. As can be seen in Fig. 1, between I_S and the measurement system, a complex impedance is always present due to the biological preparation and an electrode. The equivalent input circuit widely used in biological measurement from cells or tissues is given in Fig. 1. This input circuit can change the overall noise performance of the LCMS, therefore it is important to analyze it together with the entire measurement system. Typically, an electrode is used to access the electrical measurement from cells or tissue, and therefore an access

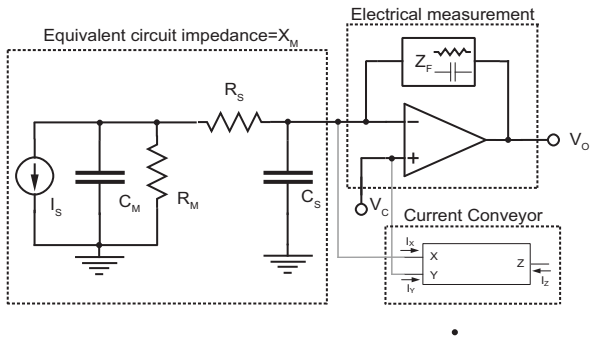

Fig. 1: Schematic diagram of the equivalent input circuit and the low current measurement system

TABLE I: Equivalent electrical input circuit values

	Cell+Pipette	Patch+Pipette	Cell+Planar	DNA
R_M	500MΩ	10GΩ	1TΩ	1GΩ
C_M	10pF	20fF	1-5fF	60pF
R_S	5MΩ	5MΩ	10MΩ	1KΩ
C_S	3pF	1pF	100-300fF	1pF

Cell+Pipette : Whole-cell recording using a micropipette [5]
Patch+Pipette : Patch clamp recording using a micropipette [5]
Cell+Planar : Whole-cell planar patch clamp recoding [6]
DNA : DNA nanopore sequencing [2]

series resistance, R_S, and parasitic capacitance, C_S, presented in the electrical equivalent input model. In parallel to I_S, a cell or tissue capacitance, C_M is present. In addition, a shunt resistance, R_M is the off resistance of the cell or tissue. Notice this directly affects the minimum current measurable, as it produces a leak shunt current. Typical values of the equivalent electrical input circuit are given in Table I.

We show the performance analysis for three kinds of LCMSs. The detailed noise analysis and performance comparison for the resistive feedback, capacitive feedback and current conveyor LCMSs are described and the measurement results from the fabricated systems are also presented.

II. Noise Analysis of Input Equivalent Circuits and LCMSs

In this section we compute the electrical noise contribution of a biosensor interface for low current measurements. Low current measurements can be performed with passive components in shunt or feedback configuration with respect to an active amplifier. For practical reasons, low current

978-1-4244-5309-2/10/$26.00 ©2010 IEEE

measurement can be conducted with capacitors or resistors in feedback configuration. Inductors can also be used for large AC currents, but are not generally employed in biosensor interfaces for their size and the small currents involved.

A. Input Equivalent Circuits

The equivalent impedance of the equivalent input circuit including various cells or tissues X_M in Fig. 1 is defined as

$$X_M = \frac{(R_M + R_S + s \cdot R_M \cdot C_M \cdot R_S)}{(1 + s \cdot (R_M \cdot C_M + C_S \cdot R_M + C_S \cdot R_S) + s^2 \cdot (R_M \cdot C_M \cdot R_S \cdot C_S))} \quad (1)$$

The power spectral density (PSD) of the thermal current noise from X_M, $S_M(f)$ can be calculated as:

$$S_M = \frac{4KT}{\mathrm{Re}\{X_M\}} \quad (2)$$

The noise spectral densities for various cells and tissues are modeled from (2) and using values in Table 1 and the simulation results are shown in Fig. 2. The input equivalent circuit not only generates noise itself, but also changes the performance of the LCMS. The noise of the DNA nanopore application has the largest noise value at higher frequencies due mainly to the large bilayer capacitance.

B. Low-Current Measurement with Resistive Feedback

The most typical continuous-time current-mode interface is a resistive feedback ($Z_F = R_F$) trans-impedance amplifier (TIA) based on an operational amplifier headstage as shown in Fig 1. The operational amplifier input configuration allows to concomitantly record input currents and clamp the input voltage, V_C. In the noise model for the LCMS with resistive feedback, the output power spectral density, S_V from the noise model of the resistor and the op-amp is given by the equations below.

$$S_V = e_R^2 + e_M^2 \cdot (1 + Y_M \cdot R_F)^2 \quad [V^2/Hz] \quad (3)$$

where e_M is the input referred noise of the op-amp, e_R is the thermal noise of the feedback resistor, R_F, and Y_M is the admittance of the equivalent input circuit (cells and tissues), X_M, defined as:

$$\begin{aligned} e_M^2 &= C_{TN} + \frac{C_{FN}}{f} \\ e_R^2 &= 4KTR_F \\ Y_M &= 1/X_M \end{aligned} \quad (4)$$

where, $C_{TN} = 8KT(\frac{2}{3 \cdot g_m})$ and $C_{FN} = \frac{2}{g_m^2}\left[\frac{K_F \cdot Id^{AF}}{C_{OX}(L_{eff}^2)}\right]$ are the thermal noise coefficient and the flicker noise coefficient of the op-amp, respectively. The measured C_{TN} and C_{FN} were 5.494×10^{-17} and 3.097×10^{-13} from the op-amp itself and these values are used in the following analysis [7].

From (3), the input referred current noise, S_I can be obtained as

$$S_I = \frac{S_V}{R_F^2} = \frac{e_M^2 + e_R^2}{R_F^2} + e_M^2 \cdot Y_M \cdot (Y_M + \frac{2}{R_F}) \quad [A^2/Hz]. \quad (5)$$

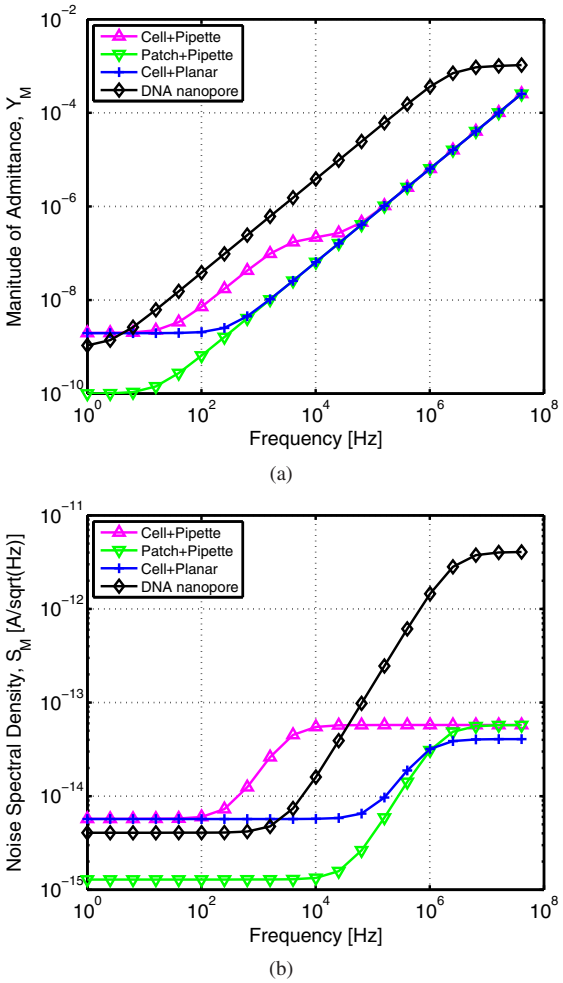

Fig. 2: Characteristics of the various cells or tissues (a) Magnitue value of the admittance, Y_M=$\frac{1}{X_M}$, (b) Noise spectral density function

S_I in (5) presents a spectral response as shown in Fig. 3. The dominant noise source at lower frequency is the feedback resistor (25MΩ) [7], and the input referred op-amp noise related the admittance of the equivalent circuit generates most of the noise in high frequency.

C. Low-Current Measurement with Capacitive Feedback

A current integrator circuit can be used for low-current integrated measurement systems with large bandwidth. The integrator is a high gain amplifier with a shunt integrating capacitor, C_F (=Z_F in Fig. 1) between its input and output terminals. The capacitor output voltage is proportional to the integration time and the input current. A typical small-size integrated capacitor is 100fF. In order to analyze the noise performance of the capacitive feedback LCMS, we need to calculate the noise for the $reset$ and $integration$ operating phases, separately.

During the $reset$ phase, the feedback capacitor's terminals are shorted. The voltage power spectral density of the output

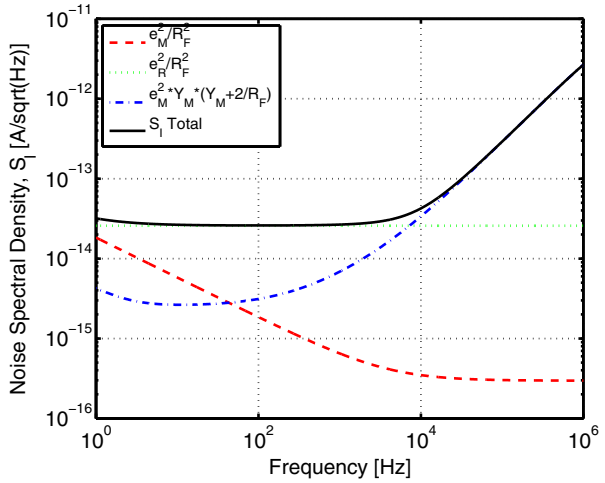

Fig. 3: Noise caused by the feedback resistor and the intrinsic op-amp noise in the resistive feedback system.

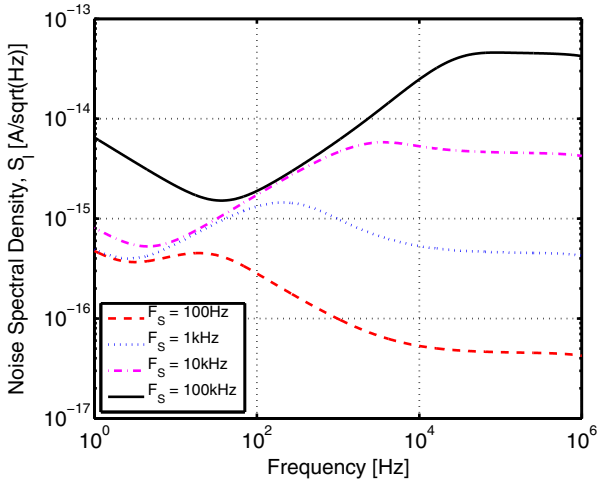

Fig. 4: Noise Spectral Density for capacitive feedback system with different sampling frequencies.

equivalent voltage noise, $S_{V,reset}$ is calculated as:

$$S_{V,reset} = e_M^2 \quad [V^2/Hz] \tag{6}$$

where e_M is the input referred noise of the op-amp, which is same with (4). The equivalent input referred current noise, $S_{I,reset}$ related with the feedback capacitance and the integration time can be obtained as:

$$S_{I,reset} = S_{V,reset} \cdot (\frac{C_F}{T_{int}})^2 = e_M^2 \cdot (\frac{C_F}{T_{int}})^2 \quad [A^2/Hz]. \tag{7}$$

During the *integration* phase, the feedback capacitor has initial charge of zero and integrates the input current. In this case, the integrated output voltage during an integration time, T_{int} can be represented by a convolution with the current and a rectangular time pulse as follows:

$$\begin{aligned} V_O(t) &= \frac{1}{C_F} \cdot \int_0^{T_{int}} i(t)\, dt \\ &= \frac{1}{C_F} \cdot i(t) * (u(t) - u(t - T_{int})). \end{aligned} \tag{8}$$

where $i(t)$ is an input current and $u(t)$ is the unit step function. Here, the Laplace transform of (8) can be obtained as:

$$\mathcal{L}(\frac{1}{C_F} \cdot i(t) * (u(t) - u(t - T_{int}))) = \frac{1}{C_F \cdot s} \cdot i(s) \cdot (1 - e^{-T_{int} \cdot s}) \tag{9}$$

where $L(i(t)) = i(s)$.

The frequency response of the capacitor integration during the finite time is a multiplication of the capacitor integration function during infinite time and the inverted exponential function. Therefore, the final frequency response is similar to a low-pass-filter. From (9), power spectral density of the output, $S_{V,int}$ is calculated as:

$$S_{V,int} = e_M^2 \cdot (\frac{Y_M}{C_F \cdot s} \cdot (1 - e^{-T_{int} \cdot s}))^2 \quad [V^2/Hz] \tag{10}$$

where e_M is the input referred noise of the op-amp. Y_M is the admittance of the equivalent input circuit, X_M.

From the above equations, the input referred current noise, $S_{I,int}$ during the integration time can be obtained as

$$\begin{aligned} S_{I,int} &= S_{I,int} \cdot (\frac{C_F}{T_{int}})^2 \\ &= e_M^2 \cdot (\frac{Y_M}{T_{int} \cdot s} \cdot (1 - e^{-T_{int} \cdot s}))^2 \quad [A^2/Hz]. \end{aligned} \tag{11}$$

For the capacitive feedback measurement system, the total input referred noise, S_I is obtained as the sum of the noise current power spectral densities of the reset phase and the integration phase ($S_{I,int}$ is dominant). Fig. 4 reports the noise spectral density with different sampling frequencies (integration times).

D. Current Conveyor

A current conveyor (amplifier) circuit in Fig. 1 is a suitable element for amplifying low current as head-stage of the LCMS and to apply voltage biases for biosensor interfaces. If a potential is applied to terminal X, the same potential appears on terminal Y, and the current flowing into terminal X will be conveyed into terminal Z with high output impedance (CCII+). The input referred current noise of CCII+ in the operation of the strong inversion can be simply represented as follows [8]

$$S_I = (8 + \frac{2}{\alpha}) \cdot (4KT\frac{2}{3}gm + \frac{K_F I d^{A_F}}{C_{OX}(L^2)f}) \quad [A^2/Hz] \tag{12}$$

where α is current amplification factor.

III. Measurement Results and Performance Comparison

Figure 5 reports the noise comparison for LCMSs and the matched measurement results from the fabricated systems. The measured noise spectral densities of the resistive feedback

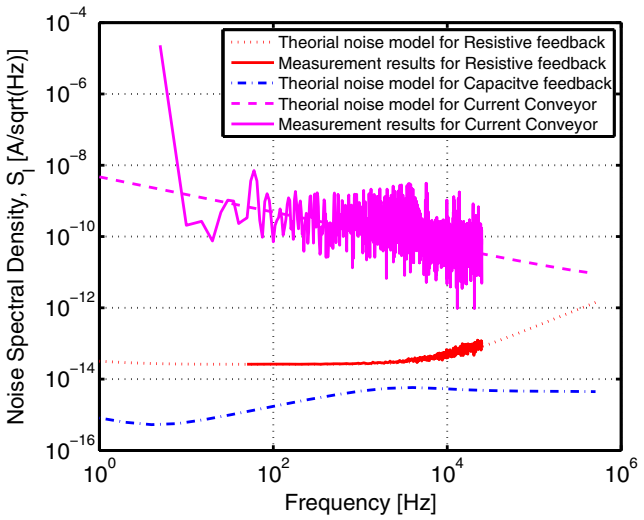

(a)

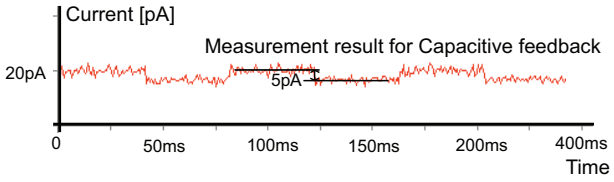

(b)

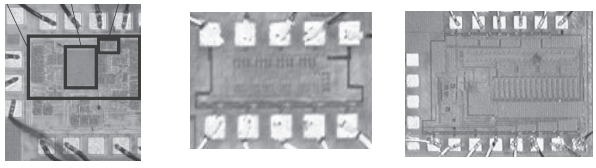

(c)

Fig. 5: Noise spectral density comparison and the matched measurement results and microphotographs of LCMSs fabricated with SOS 0.5-μm process

and the current conveyor are around 2×10^{-14} and $1.3 \times 10^{-10}[A/\sqrt{Hz}]$, respectively. RMS noise current comparison is presented in Fig. 6. The capacitive feedback system is not continuous, therefore instead of the frequency domain noise response, we provide time domain response in Fig. 5 (b). From the measurement results, we see the measured RMS noise of the capacitive feedback system is 1.4 pA RMS at 10KHz sampling rate, whereas the measured RMS noises of the resistive feedback and the current conveyor are 5pA and 750pA with the bandwidth of 10KHz, respectively. The measured RMS noises are slightly higher than the theoretical values due to the external noise sources of the test setup.

IV. Conclusion

Based on the theoretical analysis and the measurement results, the LCMS using capacitive feedback has lower noise level than the resistive feedback and the current conveyor. The

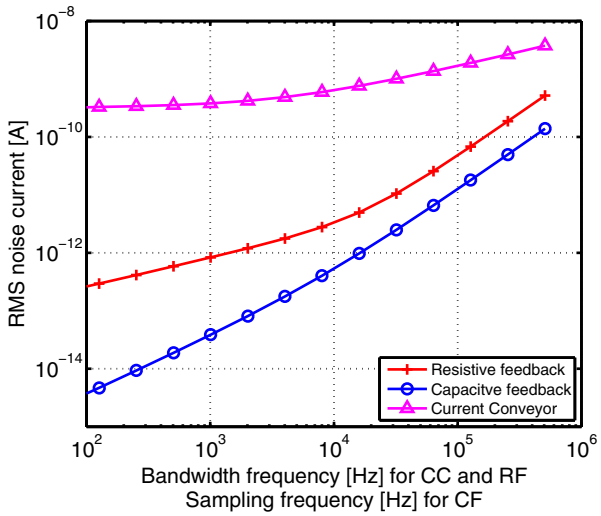

Fig. 6: RMS noise current comparison for resistive feedback, capacitive feedback, and current conveyor systems

capacitive feedback is capable of measuring 700fA RMS at 10KHz sampling rate, whereas the resistive feedback provides 4pA and the current conveyor provides 600pA. The RMS noise level can be decreased by a low pass filter with flexible bandwidth depends on the input signal frequency.

V. Acknowledgements

This project was partly funded by NSF award 0622133, ONR award N000140811014 and Peregrine Semiconductors.

References

[1] F. Sigworth and K. Klemic, "Microchip technology in ion-channel research," *IEEE Transactions On Nanobioscience*, vol. 4, pp. 121 – 127, 2005.

[2] D. Branton, D. W. Deamer, and et al, "The potential and challenges of nanopore sequencing," *Nature Biotechnology*, vol. 26, pp. 1146 – 1153, 2008.

[3] A. Yang, S. R. Jadhav, R. M. Worden, and A. J. Mason, "Compact low-power impdeance-to-digital converter for sensor array microsystems," *IEEE Journals of Solid-State Circuits*, vol. 44, no. 10, pp. 2844–2855, 2009.

[4] G. Ferrari, F. Gozzini, and M. Sampietro, "Very high sensitivity CMOS circuit to track fast biological current signals," in *IEEE Biomedical Circuits and Systems Conference, 2006. BioCAS 2006*, 2006, pp. 53–56.

[5] O. Hamill, A. Marty, E. Neher, B. Sakmann, and F. Sigworth, "Improved patch-clamp techniques for high-resolution current recording from cells and cell-free membrane patches," *Pflugers Archiv European Journal of Physiology*, vol. 391, no. 2, pp. 85–100, 1981.

[6] N. Fertig, R. Blick, and J. Behrends, "Whole cell patch clamp recording performed on a planar glass chip," *Biophysical journal*, vol. 82, no. 6, pp. 3056–3062, 2002.

[7] P. Weerakoon, K. Klemic, F. Sigworth, and E. Culurciello, "An integrated patch-clamp potentiostat with electrode compensation," *IEEE Transactions on Biomedical Circuits and Systems*, vol. 3, pp. 117–125, 2009.

[8] E. Bruun, "Analysis of the noise characteristics of CMOS current conveyors," *Analog Integrated Circuits and Signal Processing*, vol. 12, no. 1, pp. 71–78, 1997.